Performance of Wavelet Transform and Empirical Mode Decomposition in Extracting Signals Embedded in Noise

T. Kijewski-Correa[1] and A. Kareem[2]

Abstract: Time-frequency transformations have gained increasing attention for the characterization of nonstationary signals in a broad spectrum of science and engineering applications. This study evaluates the performance of two popular transformations, the continuous wavelet transform and empirical mode decomposition with Hilbert transform (EMD+HT), in estimating instantaneous frequency (IF) in the presence of noise. The findings demonstrate that under these conditions wavelets seeking harmonic similitude at various scales produce lower variance IF estimates than EMD+HT. The shortcomings of the latter approach are attributed to its empirical, envelope-dependent nature, leading to bases that are themselves derived from noise.

Introduction

A number of time-frequency transformations capable of characterizing signals with time-varying characteristics have surfaced in the literature, though two have gained popularity in the analysis of civil and mechanical systems: the continuous wavelet transform (CWT) (e.g., Kijewski and Kareem 2003) and empirical mode decomposition with Hilbert transform (EMD+HT) (Huang et al. 1998). As the performance of the former technique was called into question by Huang et al. (1998), it is important to affirm the appropriateness of CWTs for the analysis of nonstationary and nonlinear signals. Such an evaluation has already taken place in part in Kijewski-Correa and Kareem (2006, 2007) and is expanded here by evaluating the ability of EMD+HT and CWT to capture the instantaneous frequency (IF) of signals of constant and time-varying frequency in the presence of noise.

It should be immediately stated that this study evaluates the performance of the two techniques in direct application of their respective theories without the benefit of additional refinements; therefore, sophisticated CWT ridge extraction techniques (Carmona et al. 1998) and statistical confidence assessments to distinguish noise from meaningful EMD+HT data (Wu and Huang 2004) are not employed. As such, this study underscores

the inherent, fundamental limitations of the methods in the presence of noise.

Examples

The discussion herein will call upon concepts associated with the analytic signal $z(t)$ and the IF: the derivative of the analytic signal's phase (Carmona et al. 1998). The instantaneous frequency has traditionally been identified from the analytic signal generated by the Hilbert transform (HT), though this method is not capable of handling multicomponent analyses. EMD+HT and CWT have this capability, though they decompose multicomponent signals and generate the analytic signal in fundamentally different ways. In the case of EMD+HT, EMD is used to decompose the signal into its intrinsic mode functions (IMFs) and then the HT is subsequently applied to generate the analytic signal. For the CWT, an analytic parent wavelet is used (e.g., Morlet wavelet), yielding wavelet coefficients that are directly proportional to the analytic signal at the *stationary points* or ridges of the time-frequency map.

Before presenting the results, it should be emphasized that they are not achieved without a proper understanding of each approach and its implementation. For instance, it is important to note that the resolution characteristics of the Morlet wavelet analysis are dictated by the central frequency parameter f_0, according to relationships discussed in Kijewski and Kareem (2003), and greatly impact the wavelet's ability to detect nonlinear characteristics (Kijewski-Correa and Kareem 2007) and to isolate closely spaced time or frequency components (Kijewski-Correa and Kareem 2006). In this study, to preserve the capability to track time varying features, a Morlet wavelet with central frequency $f_0 = 1$ Hz is used. Larger central frequency values ($f_0 = 5$ Hz) essentially approach a Fourier-like representation (Kijewski-Correa and Kareem 2006). It should also be emphasized that EMD+HT results are presented in the form of a Hilbert spectrum, which plots the amplitude of the Hilbert-transformed IMFs as a function of time and IF. These results are compared to the wavelet instantaneous frequency spectrum (WIFS) (Kijewski-

[1]Rooney Family Assistant Professor of Engineering, Dept. of Civil Engineering and Geological Sciences, Univ. of Notre Dame, 156 Fitzpatrick Hall, Notre Dame, IN 46556 (corresponding author). E-mail: tkijewsk@nd.edu

[2]Robert M. Moran Professor of Engineering, Dept. of Civil Engineering and Geological Sciences, Univ. of Notre Dame, 156 Fitzpatrick Hall, Notre Dame, IN 46556
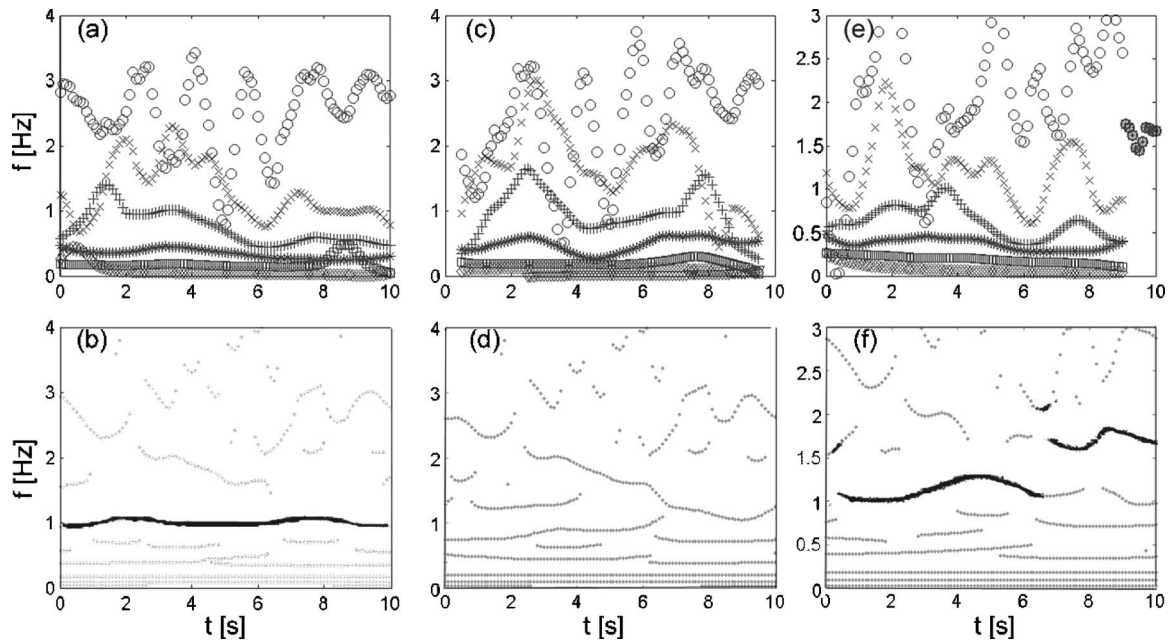
Fig. 1. *Noise-embedded sinusoid*: (a) instantaneous frequency estimate associated with each IMF; (b) skeleton plot of WIFS with most energetic component shown as darker line. *Additive white noise*: (c) instantaneous frequency estimate associated with each IMF; (d) skeleton plot of WIFS. *Noise-embedded chirp*: (e) instantaneous frequency estimate associated with each IMF; (f) skeleton plot of WIFS with most energetic component shown as darker line.

Correa and Kareem 2006), which presents a comparable representation, in contrast to the scalogram comparisons presented in Huang et al. (1998). Finally, EMD was applied under the following conditions: The maximum iteration number for each sifting was chosen as 1,000 and the number of successive sifting steps that produce the same number of extrema and zero crossings was limited to 5. Note that other sifting criteria may yield some variations in the IMFs obtained.

In the examples which follow, the signal-to-noise ratio (SNR) is defined as

$$SNR = \frac{\sigma_x}{\sigma_N} \qquad (1)$$

where σ_x=standard deviation of the signal and σ_N=standard deviation of the additive white noise drawn from a standard normal distribution. A noise embedded case (SNR < 1) will be considered as the "worst case" scenario, comparable to the noise levels investigated in other IF studies (Boashash 1992). Low-noise examples (SNR=10) are also provided so that the performance of the methods can be enveloped between two noise extremes.

Constant Frequency Sinusoid Embedded in Noise

The first noise-embedded signal is a unit amplitude, 1 Hz sinusoid (SNR=0.707). Interestingly, analysis of this signal by EMD yields 6 IMFs, while an EMD analysis of the additive noise signal by itself yielded 7 IMFs. The IMFs are omitted for brevity but can be found in Kijewski-Correa and Kareem (2005). The instantaneous frequency components associated with each IMF for the noise-embedded signal are shown in Fig. 1(a). Notice the mixing of frequency content between the first and second IMF due to EMD being ". . . as a filter bank of overlapping band-pass filters" (Flandrin et al. 2004). Other studies (Olhede and Walden 2004; Kijewski-Correa and Kareem 2005, 2006) noted the implication of such mode-mixing and its influence on the quality of estimated

IFs. For comparison, the EMD+HT analysis of the additive noise signal by itself is presented in Fig. 1(c). Notice the similarities to Fig. 1(a), with again the presence of mode mixing and a distribution of energy content over the entire time-frequency map. Thus, the 1 Hz sinusoid cannot be extracted from the large amplitude additive noise. As the sifting operation of EMD+HT is based on spline fits to envelope functions, the fact that the signal is so grossly overcome by noise implies that any decomposition based on envelope functions will likely capture only the signal components contributing to that envelope—in this case dominated by noise.

The same signal is now analyzed by CWT in Fig. 1(b). Like its Hilbert counterpart, there is a rich distribution of energy over the map, but with coefficients dominant near 1 Hz forming a continuous wavelet ridge. For comparative purposes, the same wavelet analysis is conducted on the additive noise signal by itself and the results are shown in Fig. 1(d). Note the lack of continuous ridge in the vicinity of 1 Hz and instead the sole presence of the intermittent noise distributed over the time-frequency plane. The real and imaginary components of the analytic signal extracted from this wavelet ridge are shown in Fig. 2(a). Note that the amplitude of the analytic signal is somewhat distorted due to the noise; however, the quadrature shift and thus phase is preserved. The IF estimated from the wavelet analytic signal is shown in Fig. 2(b) and its statistics are presented in Table 1.

Since no IMF captured the embedded sinusoid, an EMD +HT IF estimate for the sinusoid cannot be provided for comparison. However, the IF derived from a direct application of the HT to the noise-laden signal is provided in Fig. 2(c) for reference, and it statistics are similarly summarized in Table 1. Note the high degree of variability in the estimated IF law. Also provided for comparison is an analysis on the same sinusoid, but now under low noise (see SNR=10 in Table 1). For this low-noise case, EMD produced 5 IMFs, with the first solely carrying the extracted sinusoid, whose IF is estimated and reported in Table 1. Interest-
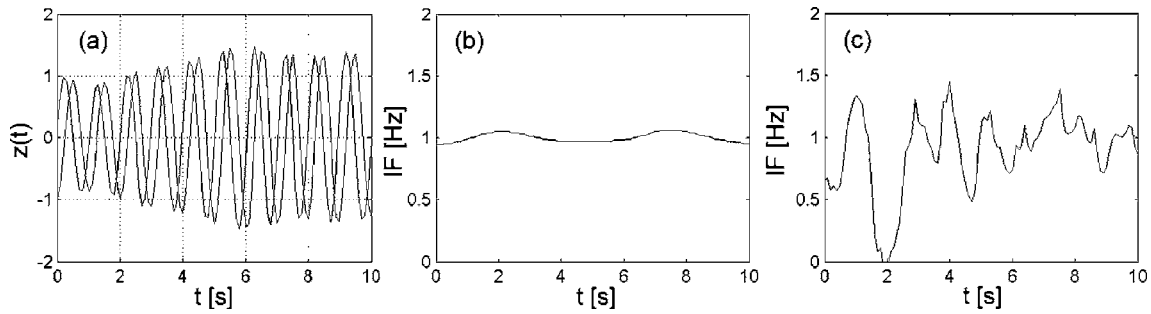
Fig. 2. Noise-embedded sinusoid: (a) CWT analytic signal components; (b) IF by CWT; and (c) IF by HT

ingly, the IF estimated from a direct application of HT to this sinusoid with SNR=10 (also provided in Table 1) performs slightly better than the EMD+HT result. This underscores the inaccuracies in the resulting IMFs, even in the presence of very low noise levels. Finally, note that the wavelet produces lesser coefficients of variation (COVs) and its mean IF shows no sensitivity to noise level.

Quadratic Chirp Embedded in Noise

To further this discussion, a quadratic chirp is now simulated with an instantaneous frequency law described by the following relationship:

$$f_{\text{chirp}}(t) = 0.01t^2 + 1 \qquad (2)$$

This signal is embedded in the same simulated random noise discussed in the previous example (SNR=0.711). The application of EMD to this noise-embedded signal produces 6 IMFs, again omitted for brevity but available in Kijewski-Correa and Kareem (2005). As in the earlier example, no singular IMF embodies the quadratic chirp, though most of the energy associated with it appears to reside in the first three IMFs. The skeleton plot of the IF associated with each IMF is shown in Fig. 1(e) and again manifests a general distribution of energy similar to the result in Fig. 1(a), with no definitive concentration of high amplitude coefficients in the vicinity of 1 to 2 Hz, where the quadratic chirp resides. The CWT analysis [Fig. 1(f)] yields high energy concentrations in the vicinity of 1 to 2 Hz, though the identified ridge does not show the same continuity as the result in Fig. 1(b) due to interferences by noise. The estimated IF law extracted from this ridge is provided in Fig. 3(a) with f_{chirp} provided for reference. Though the general quadratic trend is identified, some deviations occur at times where high concentrations of noise are concomitant with the chirp, particularly between 6 and 8 s. Again since no definitive IMF isolated the chirp, HT had to be directly applied to the signal without EMD to produce an IF law estimate. As shown in Fig. 3(b), variance of the estimated IF is larger in comparison with the wavelet result. The same simulation is repeated with

reduced amplitude noise (SNR=10). In this case, the chirp was successfully isolated by the first IMF and the extracted IF, along with its wavelet counterpart, are shown in Figs. 3(d and c), respectively. The findings are consistent with the results presented in Table 1: both methods capture the IF law in a mean sense, though variance is slightly greater for the EMD+HT result.

Discussion

The performance of EMD in the presence of noise can be explained by the fact that its sifting procedure is based upon signal envelopes that are highly distorted by noise and thus negatively impact EMD's ability to capture the embedded signal's scales. Thus, the resulting bases or IMFs are themselves derived from noise, impacting the ability to accurately isolate a frequency-modulated (FM) wave and estimate its IF with low variance. The examples herein demonstrate that analytic parent wavelets such as the Morlet wavelet are better suited to achieving high similitude with FM waves, despite the presence of large amplitude noise. The scales of signals are not impacted by noise to the same extent as signal envelopes. Thus, transforms that seek similitude in scale
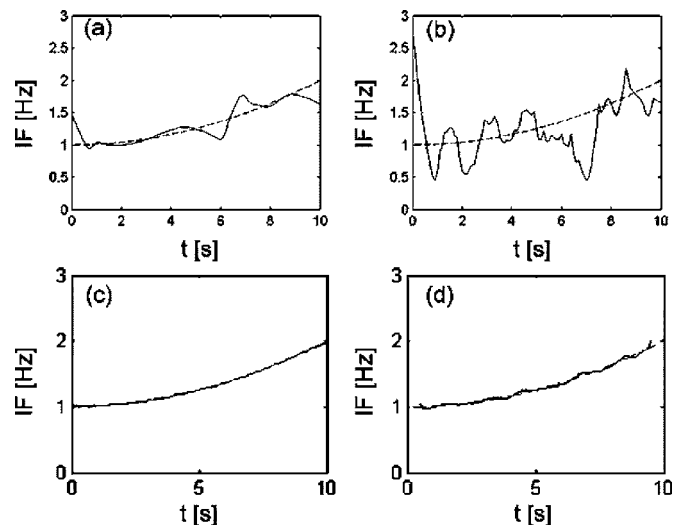
Fig. 3. Instantaneous frequency from wavelet analytic signal phase for (a) noise-embedded chirp (SNR=0.7110) and (c) noisy chirp (SNR=10); instantaneous frequency from Hilbert transform applied to (b) noise-embedded chirp (SNR=0.7110); and (d) IF extracted from first IMF of noisy chirp (SNR=10). Simulated IF law shown as dashed line in all plots.

Table 1. Mean and Coefficient of Variation of Instantaneous Frequencies of Sinusoid with Additive Noise by CWT and EMD+HT

	SNR=0.707		SNR=10	
	Mean IF (Hz)	CoV (%)	Mean IF (Hz)	CoV (%)
CWT	0.99	3.34	0.99	1.08
HT	0.90	35.8	1.00	1.48
EMD+HT	N/A	N/A	1.00	1.57

and do not derive their bases from signal envelopes perform better, explaining the superior results obtained by CWT.

Conclusions

This study provided an evaluation of CWT and EMD+HT in extracting signals embedded in both high and low noise levels. Whereas both approaches can capture the instantaneous frequency in a mean sense, irregardless of the noise level, Hilbert transform-based approaches demonstrate a higher coefficient of variation that increases with the noise level, particularly in the case of a quadratic chirp. This performance is attributed to the fact that their bases are derived from the noise-contaminated data. It was also noted that in high noise situations, there is considerable mixing of the embedded signal over the IMFs. As such, when noise is very high, a signal may not be isolated by EMD and its IF law cannot be estimated. Even in low noise simulations, IMFs were somewhat distorted and actually yielded IF estimates of higher variance than a direct application of the Hilbert transform. Thus signal extraction and reconstruction from the empirical bases of EMD+HT can be problematic as noise levels increase; thus wavelet transforms may provide a more reliable alternative for such analyses.

Acknowledgments

References

Boashash, B. (1992). "Estimating and interpreting the instantaneous frequency of a signal. 2: Algorithms and applications." *Proc. IEEE*, 80(4), 540–568.

Carmona, R., Hwang, W. L., and Torresani, B. (1998). *Practical time-frequency analysis*, 1st Ed., Academic, New York.

Flandrin, P., Rilling, G., and Gonçalvès, P. (2004). "Empirical mode decomposition as a filter bank." *IEEE Signal Process. Lett.*, 11(2, Pt 1), 112–114.

Huang, N. E., Shen, Z., Long, S. R., Wu, M. C., Shih, H. H., Zheng, Q., Yen, N.-C., Tung, C. C., and Lu, H. H. (1998). "The empirical mode decomposition and the Hilbert spectrum for nonlinear and nonstationary time series analysis." *Proc.: Mathematical, Physical, and Engineering Sci.*, 454(1971), 903–995.

Kijewski, T., and Kareem, A. (2003). "Wavelet transforms for system identification in civil engineering." *Comput. Aided Civ. Infrastruct. Eng.*, 18(5), 341–357.

Kijewski-Correa, T., and Kareem, A. (2006). "Efficacy of Hilbert and wavelet transforms for time-frequency analysis." *J. Eng. Mech.*, 132(10), 1037–1049.

Kijewski-Correa, T., and Kareem, A. (2007), "Nonlinear signal analysis: Time-frequency perspectives." *J. Eng. Mech.*, 133(2), 238–245.

Kijewski-Correa, T. L., and Kareem, A. (2005). "Efficacy of Hilbert and wavelet transforms for time-frequency analysis." *Proc., Int. Conf. on Structural Safety and Reliability*, International Association for Structural Safety and Reliability, Univ. degli Studi di Roma "La Sapienza," Rome, Italy.

Olhede, S., and Walden, A. T. (2004). "The Hilbert spectrum via wavelet projections." *Proc. R. Soc. London, Ser. A*, 460(2044), 955–975.

Wu, Z., and Huang, N. E. (2004). "A study of the characteristic of white noise using the empirical mode decomposition method." *Proc. R. Soc. London, Ser. A*, 460(2046), 1597–1611.